

Effective Additives of A (Ce, Pr) in Modified Hexaaluminate $\text{La}_x\text{A}_{1-x}\text{NiAl}_{11}\text{O}_{19}$ for Carbon Dioxide Reforming of Methane

Ke Zhang · Guangdong Zhou · Jing Li ·
Kaiji Zhen · Tiexin Cheng

Received: 8 November 2008 / Accepted: 22 January 2009 / Published online: 14 February 2009
© Springer Science+Business Media, LLC 2009

Abstract A study on Pr or Ce modified hexaaluminates, $\text{La}_x\text{A}_{1-x}\text{NiAl}_{11}\text{O}_{19}$ ($x = 0.8$) and $\text{LaNiAl}_{11}\text{O}_{19}$ as catalysts for carbon dioxide reforming of methane was carried out by means of XRD, TGA, XPS and TPR techniques. The experimental results indicate that the catalytic properties of the $\text{La}_{0.8}\text{Pr}_{0.2}\text{NiAl}_{11}\text{O}_{19}$ are more optimal than those of the $\text{La}_{0.8}\text{Ce}_{0.2}\text{NiAl}_{11}\text{O}_{19}$. These catalysts were studied in more detail and it was found that the active nickel phase strongly depends on the interactions of the Ni ion and the La ion, which are related to the additives (Ce, Pr).

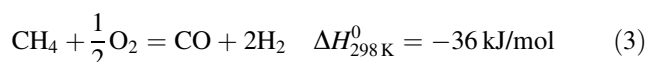
Keywords Hexaaluminate $\text{La}_x\text{A}_{1-x}\text{NiAl}_{11}\text{O}_{19}$ · Methane · CO_2 reforming · Catalysis · Synthesis gas

1 Introduction

CH_4 reforming with CO_2 has attracted much attention since the past years due to utilization of these two cheapest carbon-containing compounds to syngas ($\text{CO} + \text{H}_2$) [1]. Equation 1 represents conversion of the major greenhouse gas, CO_2 , into the synthesis gas through the reforming reaction of methane,



The reforming products CO and H_2 with equal molar ratio are more suitable for the subsequent Fischer–Tropsch synthesis compared to the products of the steam reforming Eq. 2 or partial oxidation of methane Eq. 3 [2].



In the environmental aspect, both CO_2 and methane are undesirable greenhouse gases, and the reforming reaction provides a way for CO_2 utilization [3]. The reforming reaction can be utilized to produce valuable feedstock for chemical industry.

Precious metals Rh, Ru, Pd, Pt and Ir have successfully been employed as highly active catalysts for CO_2 reforming of methane to synthesis gas [4, 5]. However, the high cost and limited availability of the noble metals have stimulated researching for cheaper metals such as ferrous metals (Fe, Co and Ni) as worthwhile alternatives to the noble metals [6]. Ni-based catalysts with lower cost are highly active for the catalytic dry reforming and plentifully available compared to the noble metal catalysts [7]. Although supported Ni-based material has been reported to be an effective catalyst for this reaction, it suffers a serious problem: deactivation due to carbon deposition, nickel sintering and phase transformation of the catalyst [4]. Therefore, it is very important to improve the state of supported Ni catalysts in order to overcome these disadvantages. Some researchers have made efforts to enhance the catalytic activity and stability of the Ni-based catalysts by using different supports, promoters and nickel precursor compounds [8–11].

Iyi et al. studied the hexaaluminate crystal structure in detail [12]. Every hexaaluminate compound crystallizes in either $\beta\text{-Al}_2\text{O}_3$ or magnetoplumbite structure. Both of these structures consist of alternative stacking of a spinel block and a mirror plane; in addition, the structure type of hexaaluminates depends on the charge and radius of the large modification cations in the mirror plane layer. Some

K. Zhang · G. Zhou · J. Li · K. Zhen · T. Cheng (✉)
College of Chemistry, Jilin University, 130023 Changchun,
People's Republic of China
e-mail: ctx@mail.jlu.edu.cn

hexaaluminates have been reported to be good catalysts for high-temperature catalytic combustion [13, 14]. Up to date, few papers concerning Ni substituted hexaaluminate used as catalyst for the topic reaction have been published [15, 16].

There have been two series of hexaaluminates $\text{ANiAl}_{11}\text{O}_{19-\delta}$ ($A = \text{Ca, Sr, Ba, and La}$) and $\text{LaNi}_y\text{Al}_{12-y}\text{O}_{19-\delta}$ ($y = 0.3, 0.6, 0.9, \text{ and } 1.0$) reported as a new generation of catalysts for CO_2 reforming of methane to synthesis gas [17, 18]. Interaction of Ni particles and crystalline structure can stabilize small Ni crystallites and increase catalyst life time due to decreasing carbon deposition. Whereafter Yan prepared $\text{La}_{0.8}\text{Pr}_{0.2}\text{NiAl}_{11}\text{O}_{19}$ to substitute part of La ion by Pr ion, which exhibited effective catalytic activity and stability, respectively, for 300 h of time on stream and even longer [19].

In order to find out the reason of higher activity of these catalysts, the present work describes a simple preparation method of rare earth metal modified hexaaluminates $\text{La}_{0.8}\text{A}_{0.2}\text{NiAl}_{11}\text{O}_{19}$ ($A = \text{Ce, Pr}$), in which Ni ions as active component are inlaid in the hexaaluminate lattices to substitute part of Al ions. Various hexaaluminates catalysts including $\text{La}_{0.8}\text{A}_{0.2}\text{NiAl}_{11}\text{O}_{19}$ ($A = \text{Ce, Pr}$) and $\text{LaNiAl}_{11}\text{O}_{19}$ were characterized in which the rare earth metal such as Pr and Ce were used as promoters. The effects of these modifiers on hexaaluminates catalyst were also characterized by TPR, TGA, XRD and XPS to evaluate several important factors for the high catalytic properties of these catalysts.

2 Experimental

2.1 Catalysts Preparation and Characterization

Both the Pr and Ce modified hexaaluminate catalysts, $\text{La}_x\text{A}_{1-x}\text{NiAl}_{11}\text{O}_{19}$ ($x = 0.8$) used in this research, were prepared as follows: cerium, praseodymium and lanthanum nitrates, $\text{Ni}(\text{NO}_3)_2 \cdot 6\text{H}_2\text{O}$ and $\text{Al}(\text{NO}_3)_3 \cdot 9\text{H}_2\text{O}$ were dissolved in distilled water with a molar ratio of 0.2:0.8:1:11, respectively, and the $\text{LaNiAl}_{11}\text{O}_{19}$ was prepared as described below: lanthanum nitrates, $\text{Ni}(\text{NO}_3)_2 \cdot 6\text{H}_2\text{O}$ and $\text{Al}(\text{NO}_3)_3 \cdot 9\text{H}_2\text{O}$ were dissolved in distilled water with a molar ratio of 1:1:11. Then the aqueous solutions were slowly added to a polyethylene glycol–isopropyl alcohol solution under magnetically stirring. The mixture solution was evaporated at 80 °C to dry, and stored in an oven to remove polyethylene glycol and to decompose the nitrates. After being ground into fine powder, the samples were calcined at 400 °C for 2 h, followed by calcination at 1,250 °C for 5 h.

The crystal structure of the calcined samples was determined by X-ray powder diffraction (XRD; Shimadzu

XD-3A diffractometer) using a Ni filter and Cu $K\alpha$ radiation, at 30 kV and 20 mA. Diffraction peaks recorded (for the 2° value range) between 10° and 80° are used to identify the structure of the catalysts.

The binding energy of different ions on the surface of the catalysts was measured by X-ray photoelectron spectroscopy (XPS; V.G. ESCA Mark II) using Al $K\alpha$ radiation. The measurements were operated at a pass energy of 50 eV and a step size of 0.05 eV.

The amount of carbon deposited on the catalysts was determined by oxidation conducted using a thermogravimetric analyzer (TGA; Perkin–Elmer TGA7).

The reducibility of the hexaaluminates $\text{LaNiAl}_{11}\text{O}_{19}$ and $\text{La}_{0.8}\text{A}_{0.2}\text{NiAl}_{11}\text{O}_{19}$ ($A = \text{Ce, Pr}$) was characterized by temperature-programmed reduction technique (TPR). For this purpose 0.1 g of catalyst was embedded in a fixed-bed quartz tube with an inner diameter of 4 mm in each run. Before the reduction, the sample was treated at 300 °C for 30 min and cooled to room temperature in Ar flow. Then, the reactor was heated from room temperature to 1,200 °C at a linear heating rate of 7 °C/min in a 5% H_2/Ar mixture gas flow at a rate of 30 ml/min. The temperature was measured using a thermocouple located in the bed and the effluent gases were passed through a dryer filled with 5A molecular sieve. A gas chromatograph (Shimadzu GC-8A) equipped with a thermal conductivity detector (TCD) was employed.

2.2 Catalytic Properties Test

The reforming reaction was carried out under atmospheric pressure in a tubular fixed-bed quartz reactor. A thermocouple was placed in the center of the catalyst bed to monitor the reaction temperature. The reactant mixture consisted of CH_4 and CO_2 with a molar ratio of 1:1 and was fed at a rate of 30 ml/min. About 0.3 g of catalyst was embedded in the reactor with an inner diameter of 8 mm. Before reaction, the catalyst was reduced at 900 °C in a flow of 10% H_2/Ar mixture gas for 40 min. The exit gases (reactant/product mixtures) were analyzed by a gas chromatograph (Shimadzu GC-8A) equipped with a thermal conductivity detector (TCD) and Porapak-Q and 5A molecular sieve columns. The catalytic activities were investigated at temperatures ranging from 500 to 800 °C.

3 Results and Discussion

3.1 Thermodynamics of Carbon dioxide Reforming of Methane

Carbon dioxide reforming of methane is a highly endothermic reaction (Eq. 1). Thermodynamic calculation

indicates that this reaction (Eq. 1) under 1 atmospheric pressure and below 633 °C is not spontaneous (i.e., $\Delta G > 0$). However, at high temperatures the reforming reaction takes place spontaneously, however four side reactions (Eqs. 4–7) may occur, which have a significant impact on the target reaction (Eq. 1) [20].

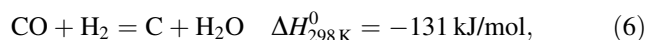
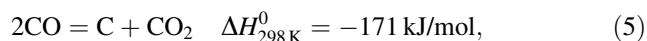
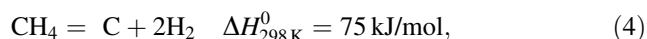


Figure 1 shows variation of equilibrium constants of the four side reactions as a function of temperature. For the strong endothermic reaction, the equilibrium constant of Eq. 1 increases dramatically with increasing temperature. Thus, high conversion can be obtained at high temperatures. The equilibrium constants of the moderate endothermic reactions [methane decomposition (Eq. 4) and the reverse water-gas shift reaction (RWGS; Eq. 7)] also increase with temperature. The two carbon deposition reactions [the Boudouard reaction (Eq. 5) and the reverse carbon gasification reaction (Eq. 6)] are exothermic and thermodynamically unfavorable at high temperatures. Therefore, high reaction temperatures (i.e., 750 °C and even higher) are more favorable to increasing the equilibrium conversion of the target reaction (Eq. 1).

3.2 Catalytic Activity

The influence of temperature on the reduced hexaaluminate $\text{La}_{0.8}\text{A}_{0.2}\text{NiAl}_{11}\text{O}_{19}$ catalysts can be seen in Fig. 2. The

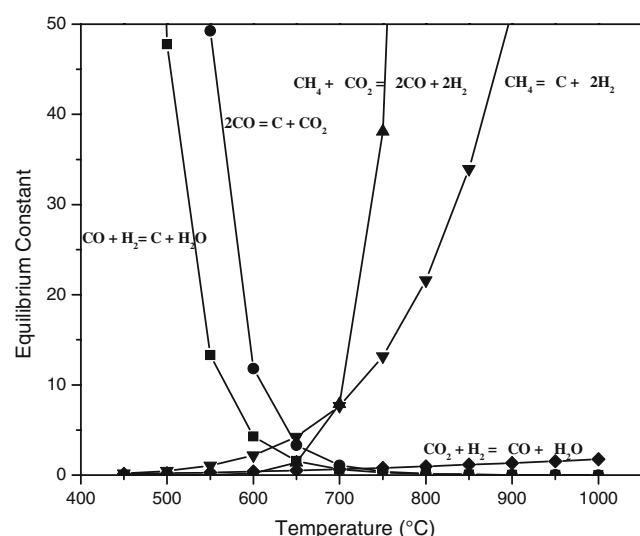


Fig. 1 Equilibrium constants of reactions (Eqs. 1, 4–7) as a function of temperature

catalytic activities of the reduced $\text{La}_{0.8}\text{A}_{0.2}\text{NiAl}_{11}\text{O}_{19}$ for the reaction in a temperature range between 500 and 800 °C indicate that the conversions of both CH_4 and CO_2 rapidly increased with increasing temperature and over 90% of their conversion was reached at 800 °C, meaning that hexaaluminates $\text{La}_{0.8}\text{A}_{0.2}\text{NiAl}_{11}\text{O}_{19}$ are significantly active for this reaction.

Table 1 gives the catalytic activities of the $\text{La}_{0.8}\text{A}_{0.2}\text{NiAl}_{11}\text{O}_{19}$ ($\text{A} = \text{Ce}, \text{Pr}$) and $\text{LaNiAl}_{11}\text{O}_{19}$ under the reaction conditions. It can be seen that the Pr modified catalyst exhibits effective catalytic activity. The activity sequence of the reduced hexaaluminates is $\text{La}_{0.8}\text{Pr}_{0.2}\text{NiAl}_{11}\text{O}_{19} > \text{LaNiAl}_{11}\text{O}_{19} > \text{La}_{0.8}\text{Ce}_{0.2}\text{NiAl}_{11}\text{O}_{19}$. As shown in Table 1, the $\text{La}_{0.8}\text{Pr}_{0.2}\text{NiAl}_{11}\text{O}_{19}$ provides 89.62 and 92.94% conversion of CH_4 and CO_2 , respectively, which approach the equilibrium ones of the reaction [21].

The amount of carbon deposited on the reduced hexaaluminates $\text{LaNiAl}_{11}\text{O}_{19}$ and $\text{La}_{0.8}\text{A}_{0.2}\text{NiAl}_{11}\text{O}_{19}$ ($\text{A} = \text{Ce}, \text{Pr}$) reached 1.4, 1.2 and 0.78 wt% (for 2 h), respectively, and no Ni sintering and phase transformation are found. These data show that rare-earth metal cation has significantly ability of restraining carbon deposition and provides a main reason for the significantly catalytic activities and stability of $\text{La}_{0.8}\text{A}_{0.2}\text{NiAl}_{11}\text{O}_{19}$ ($\text{A} = \text{Ce}, \text{Pr}$) and $\text{LaNiAl}_{11}\text{O}_{19}$ catalysts. The activity sequence of the reduced hexaaluminates illuminates that the stability and catalytic activity of $\text{La}_{0.8}\text{A}_{0.2}\text{NiAl}_{11}\text{O}_{19}$ are sensitively affected by modifier Pr or Ce.

3.3 Crystal Structure and Stability of Hexaaluminates

$\text{La}_{0.8}\text{A}_{0.2}\text{NiAl}_{11}\text{O}_{19}$

Figure 3 shows the XRD patterns of hexaaluminates $\text{LaNiAl}_{11}\text{O}_{19}$ and $\text{La}_{0.8}\text{A}_{0.2}\text{NiAl}_{11}\text{O}_{19}$ ($\text{A} = \text{Ce}, \text{Pr}$) before reduction. It is found that the series of samples exhibit almost the same hexaaluminate crystalline structure: the characteristic diffraction peaks of $\text{LaNiAl}_{11}\text{O}_{19}$ and $\text{La}_{0.8}\text{A}_{0.2}\text{NiAl}_{11}\text{O}_{19}$ ($\text{A} = \text{Ce}, \text{Pr}$) are all at 35.9, 33.8 and 31.9°. The crystalline structure of the hexaaluminates obtained is consistent with that of the samples synthesized by the hydrolysis of metal alkoxides method and the aerogel-derived approach reported in [15, 22–24].

Figure 4 is XRD patterns of hexaaluminates $\text{LaNiAl}_{11}\text{O}_{19}$ and $\text{La}_{0.8}\text{A}_{0.2}\text{NiAl}_{11}\text{O}_{19}$ ($\text{A} = \text{Ce}, \text{Pr}$) after reduction. A peak of metallic $\text{Ni}^0(111)$ at 44.5° can be clearly seen in the patterns of the samples after reduction. Besides, there is no difference in the structure of catalyst between after and before reduction, indicating that a large fraction of metallic Ni^0 is exsited on the hexaaluminate phase to form individual metallic phase, which is the active component for the reaction. These data indicate that the reduction of Ni^{2+} of hexaaluminate crystalline doesn't damage the crystalline structure of the sample.

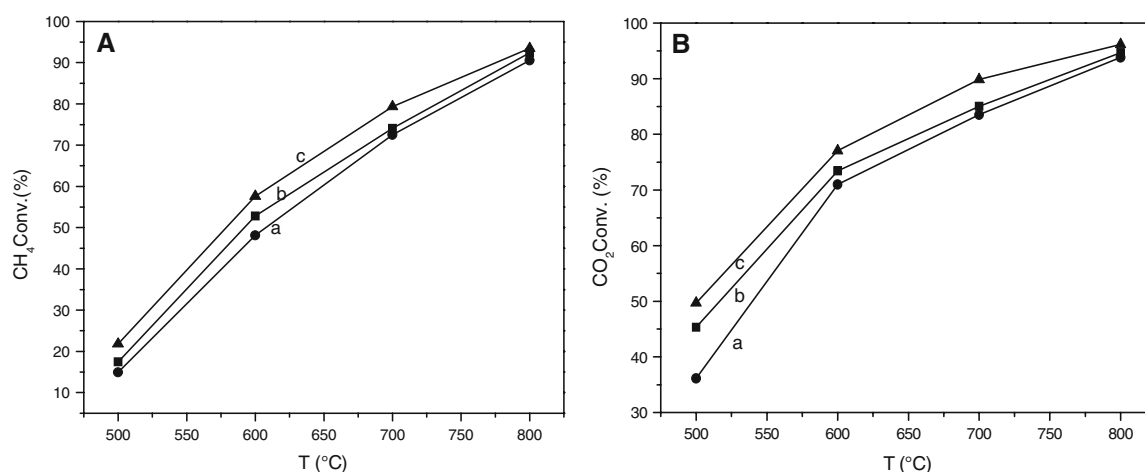


Fig. 2 Temperature dependence of the conversions of CH_4 (a) and CO_2 (b) over the reduced hexaaluminates $\text{La}_{0.8}\text{A}_{0.2}\text{NiAl}_{11}\text{O}_{19}$: 9 (a) $\text{La}_{0.8}\text{Ce}_{0.2}\text{NiAl}_{11}\text{O}_{19}$ (b) $\text{LaNiAl}_{11}\text{O}_{19}$ (c) $\text{La}_{0.8}\text{Pr}_{0.2}\text{NiAl}_{11}\text{O}_{19}$, $V(\text{CH}_4):V(\text{CO}_2) = 1:1$, flow rate 30 ml/min, catalyst 0.3 g

Table 1 Catalytic activities of the $\text{LaNiAl}_{11}\text{O}_{19}$ and $\text{La}_{0.8}\text{A}_{0.2}\text{NiAl}_{11}\text{O}_{19}$ (A = Ce, Pr)

Catalyst	Conversion (%)		Selectivity (%)		Distribution of products (%)				$n\text{H}_2/n\text{CO}$
	CH_4	CO_2	CO	H_2	H_2	CO	CH_4	CO_2	
$\text{LaNiAl}_{11}\text{O}_{19}$	82.60	90.00	50.33	50.94	45.98	46.58	4.87	2.57	0.99
$\text{La}_{0.8}\text{Ce}_{0.2}\text{NiAl}_{11}\text{O}_{19}$	72.39	90.91	51.84	51.80	42.99	46.27	8.51	2.23	0.93
$\text{La}_{0.8}\text{Pr}_{0.2}\text{NiAl}_{11}\text{O}_{19}$	89.62	92.94	50.06	50.44	47.66	47.77	2.76	1.81	1.00

Reaction conditions: $P = 0.1$ MPa, $\text{GHSV} = 9,000 \text{ h}^{-1}$, $V_{\text{CO}_2}/V_{\text{CH}_4} = 1$, $t = 120$ min, $T = 1,023$ K

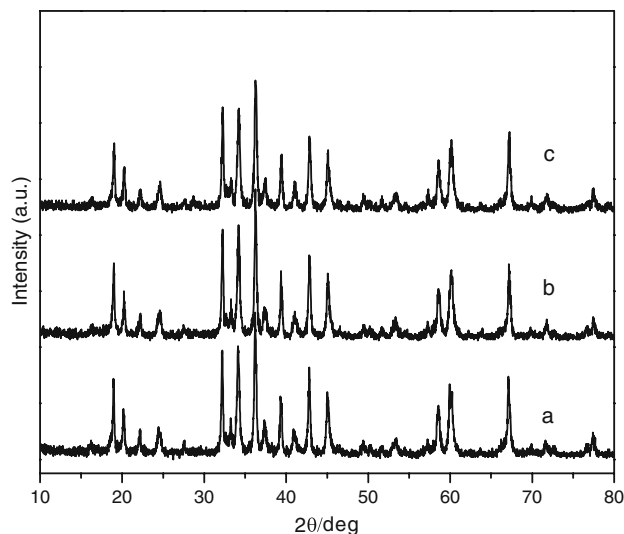


Fig. 3 XRD patterns of $\text{LaNiAl}_{11}\text{O}_{19}$ and $\text{La}_{0.8}\text{A}_{0.2}\text{NiAl}_{11}\text{O}_{19}$ (A = Ce, Pr) before reduction. a. La, b. Pr, c. Ce

From Fig. 5, it can be observed that XRD patterns of hexaaluminates $\text{LaNiAl}_{11}\text{O}_{19}$ and $\text{La}_{0.8}\text{A}_{0.2}\text{NiAl}_{11}\text{O}_{19}$ (A = Ce, Pr) remained unchanged and no Ni sintering and phase transformation are found after the reforming reaction for 2 h. However, compared to $\text{La}_{0.8}\text{Pr}_{0.2}\text{NiAl}_{11}\text{O}_{19}$ at 44.5° in the XRD patterns of $\text{Ni}^0(111)$ before reaction, a

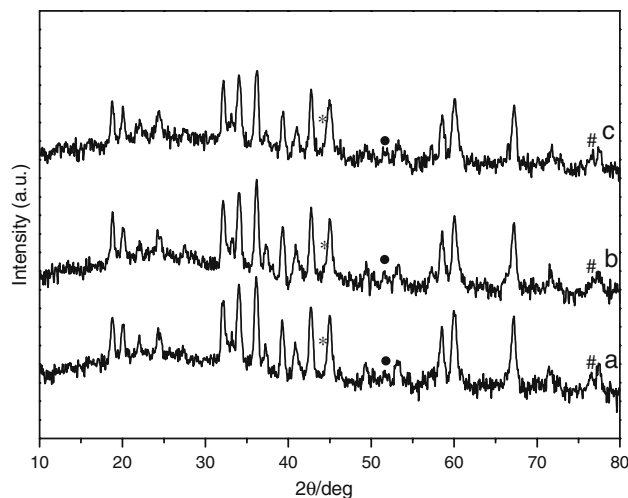


Fig. 4 XRD patterns of $\text{LaNiAl}_{11}\text{O}_{19}$ (a) and $\text{La}_{0.8}\text{A}_{0.2}\text{NiAl}_{11}\text{O}_{19}$ (b, c, Pr) after reduction * Ni (111), ● Ni (200), # Ni (220)

0.04° shift of 2θ towards higher angle and a weak intensity of the peak for $\text{Ni}^0(111)$ can be observed (inset of Fig. 5) in the XRD patterns of $\text{Ni}^0(111)$ after reaction. Appearance of this phenomenon may be directly attributed to $\text{Ni}(\text{C})$ according to Ase Slagtern [25]. This result owes to dissolution of some carbon atoms (or species) into the nickel crystallite, which weakens the XRD patterns of Ni^0 .

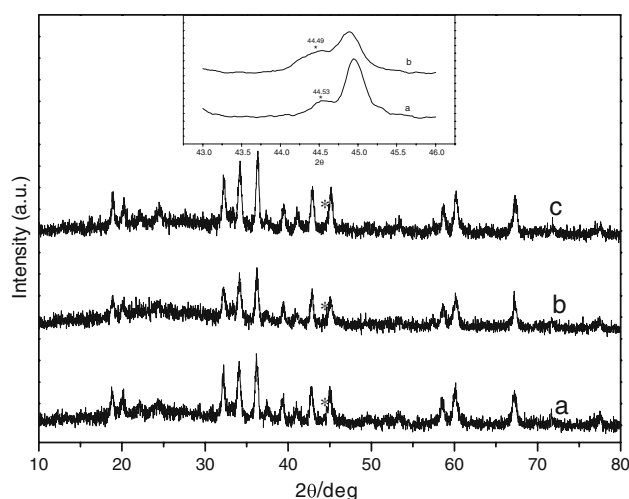


Fig. 5 XRD patterns of $\text{LaNiAl}_{11}\text{O}_{19}$ (a) and $\text{La}_{0.8}\text{A}_{0.2}\text{NiAl}_{11}\text{O}_{19}$ (b, c, Pr) after reaction for 2 h. Inset: $\text{La}_{0.8}\text{Pr}_{0.2}\text{NiAl}_{11}\text{O}_{19}$ (a) before reaction and (b) after reaction for 2 h

These results confirm that the structure of hexaaluminates is extremely stable after reaction at high temperature and the reduction. The positions and the intensities of the peaks of this series of catalysts are still the same as that measured before reaction, and only a part of Ni^{2+} ions in the hexaaluminate lattices can be reduced to Ni^0 (44.5°) under the reduction by hydrogen and the crystalline structure has not been changed even at high temperature after reduction. And the reduction degree of Ni^{2+} is also effected by rare earth modifiers. But after reaction, it can be induced to be weakened by some carbons deposited.

3.4 Oxidation State and Chemical Composition of Surface Elements

Table 2 gives the binding energy of the elements on the surface of hexaaluminates $\text{LaNiAl}_{11}\text{O}_{19}$ and $\text{La}_{0.8}\text{A}_{0.2}\text{NiAl}_{11}\text{O}_{19}$ (A = Ce, Pr) before reduction. It can be seen that the binding energies of Al and O on the surface are not affected by rare earth ions, meaning that their valence state on the surface does not change in the rare earth ion modified samples. Thus, based upon the binding energy, it can be concluded that there exist La^{3+} , Al^{3+} and O^{2-} ,

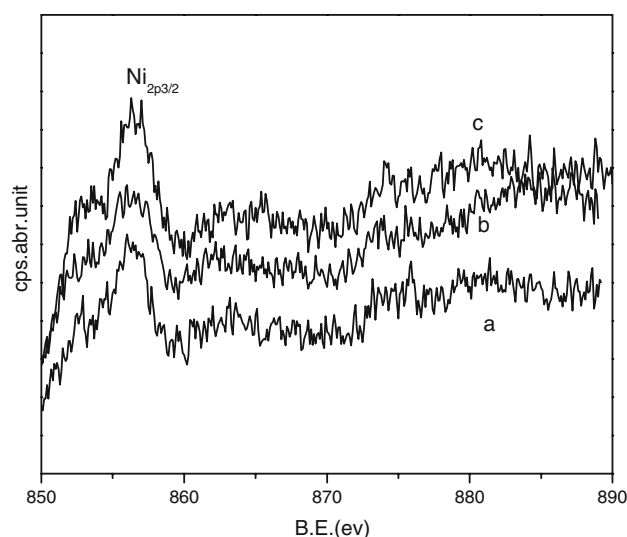


Fig. 6 XPS spectra of Ni on the surface of hexaaluminates $\text{LaNiAl}_{11}\text{O}_{19}$ and $\text{La}_{0.8}\text{A}_{0.2}\text{NiAl}_{11}\text{O}_{19}$ (A = Ce, Pr) before reduction A: a. Pr, b. Ce, c. La

respectively. From the XPS spectra of Ni on the surface (Fig. 6), it is observed that the position of $\text{Ni}_{2p_{3/2}}$ peak does not remain unchanged, namely, due to the effect of the modifiers the binding energy of Ni in the hexaaluminates $\text{La}_{0.8}\text{A}_{0.2}\text{NiAl}_{11}\text{O}_{19}$ (A = Ce, Pr) has been changed before reduction. It is concluded that Ce and Pr have been entered in the hexaaluminate crystalline structure to replace a part of La ions, and affected Ni on the surface. Although all the binding energy of Ni of hexaaluminates $\text{LaNiAl}_{11}\text{O}_{19}$ and $\text{La}_{0.8}\text{A}_{0.2}\text{NiAl}_{11}\text{O}_{19}$ (A = Ce, Pr) are slightly different before reduction, they are all located at about 856.0 eV for all of the samples. According to the attribution of $\text{Ni}_{2p_{3/2}}$ at 856.0 eV, the oxidation state of the Ni ions on the hexaaluminate lattices is Ni^{2+} . Zhanlin Xu et al. [26] also attributed the 856.2 eV peak to Ni^{2+} state for hexaaluminate $\text{LaNiAl}_{11}\text{O}_{19}$ catalyst. Generally, the binding energy of $\text{Ni}_{2p_{3/2}}$ in pure NiO is about 853.6 eV and in NiAl_2O_4 is about 856.6 eV [27]. The binding energy of $\text{Ni}_{2p_{3/2}}$ of all the samples is higher than 853.6 eV. The increase in the binding energy of $\text{Ni}_{2p_{3/2}}$ indicates that the Ni species do not exist as NiO and there exists strong interaction between Ni and La. Shuben Li et al. [28] suggested that the nickel

Table 2 XPS datas of $\text{LaNiAl}_{11}\text{O}_{19}$ and $\text{La}_{0.8}\text{A}_{0.2}\text{NiAl}_{11}\text{O}_{19}$ (A = Ce, Pr) before or after CH_4 reforming with CO_2

Sample	$\text{Ni}_{2p_{3/2}}$ (eV)		$\text{La}_{3d_{5/2}}$ (eV)	$\text{Pr}_{3d_{5/2}}$ (eV)	$\text{Ce}_{3d_{5/2}}$ (eV)		O1 s (eV)	$\text{Al}_{2p_{3/2}}$ (eV)
Fresh $\text{La}_{0.8}\text{Pr}_{0.2}\text{NiAl}_{11}\text{O}_{19}$	856.4	—	834.5	940.8	—	—	530.7	74.1
Used $\text{La}_{0.8}\text{Pr}_{0.2}\text{NiAl}_{11}\text{O}_{19}$	854.1	852	836.0	932.8	—	—	530.9	74.2
Fresh $\text{LaNiAl}_{11}\text{O}_{19}$	855.3	—	834.9	—	—	—	530.7	74.1
Used $\text{LaNiAl}_{11}\text{O}_{19}$	854.8	852.3	835.1	—	—	—	530.9	74.2
Fresh $\text{La}_{0.8}\text{Ce}_{0.2}\text{NiAl}_{11}\text{O}_{19}$	855.9	—	834.7	—	—	882.8	530.7	74.1
Used $\text{La}_{0.8}\text{Ce}_{0.2}\text{NiAl}_{11}\text{O}_{19}$	854.5	851.5	835.3	—	884.4	881.7	530.6	74.2

species with a $\text{Ni}_{2p_{3/2}}$ peak at a binding energy of 856 eV and the accompanying shake-up satellite peak at 862 eV are characterized for NiAl_2O_4 . The crystal structure of hexaaluminate belongs to β -alumina or magnetoplumbite structure. Both of these structures consist of alternative stacking of a spinel block and a mirror plane [29]. The hexaaluminate possesses a formula, $\text{LaNiAl}_{11}\text{O}_{19}$ and $\text{La}_{0.8}\text{A}_{0.2}\text{NiAl}_{11}\text{O}_{19}$ ($\text{A} = \text{Ce}, \text{Pr}$), in which one Al ion per double spinel block is replaced by one Ni ion; therefore, the Ni ion in the hexaaluminate is actually present in the lattices of the spinel block such as ' NiAl_2O_4 '. The binding energy of the $\text{Ni}_{2p_{3/2}}$ on the surface of hexaaluminate is similar to that of $\text{Ni}_{2p_{3/2}}$ in NiAl_2O_4 . Therefore, it is reasonable to attribute the peak at 856.0 eV to Ni^{2+} ions for the hexaaluminate $\text{La}_{0.8}\text{A}_{0.2}\text{NiAl}_{11}\text{O}_{19}$, which indicates that the valence state of the Ni ions on the surface is the same, and is not changed by the modifiers.

As shown in Table 2, the binding energies of O_{1s} and $\text{Al}_{2p_{3/2}}$ on the surface of the samples do not change before and after the reaction, but after the reforming reaction the binding energies of $\text{Ni}_{2p_{3/2}}$ in these used catalysts are less than that in the fresh catalysts at Ni^{2+} (856 eV) of NiAl_2O_4 . Simultaneously, there exists Ni^0 (852 eV) and the binding energies of $\text{La}_{3d_{5/2}}$ in these catalysts increases after reaction. These data show that electrons are transferred from La to Ni to maintain Ni at a lower valence, which promotes the activation of CH_4 [30]. At the same time, the binding energies of $\text{La}_{3d_{5/2}}$ increases by 1.5 eV in $\text{La}_{0.8}\text{Pr}_{0.2}\text{NiAl}_{11}\text{O}_{19}$ while those of $\text{La}_{0.8}\text{Ce}_{0.2}\text{NiAl}_{11}\text{O}_{19}$ are increased by 0.6 eV. It is indicated that the modifier Pr has an effect on La, which can enhance transformation of electrons between La and Ni. From the data, it can be assumed that the effect of modifier Ce on the transformation of electrons is less than that of Pr, which may be due to the appearance of some Ce^{3+} (884.4 eV) after reaction through the redox of $\text{Ce}^{4+}/\text{Ce}^{3+}$ [31]. The electron transformation between Ce^{4+} and Ce^{3+} may reduce the effect on electron transformation between La and Ni, as a result, the influence of Ce is weakened for La.

The above mentioned result reveals that during the reaction the main valence state of nickel is its oxidative form Ni^{2+} , part of which can be completely reduced to Ni^0 under the reduction conditions. In addition, because of the electron transformation between La and Ni, Ni can remain in its lower valence state. Moreover the effect of modifier Pr for La can intensify the electron transformation and is stronger than Ce.

The XPS data of Ni ($2p_{3/2}$) for all the catalysts after reduction are displayed in Fig. 7. Compared with Fig. 6, it is evident that there is Ni^0 (852.4 eV) on these catalysts besides Ni^{2+} (856.3 eV). This result illuminates that a part of Ni^{2+} ions is out of the crystal lattice through reduction by H_2 . As a result, these catalysts contain all the two types of

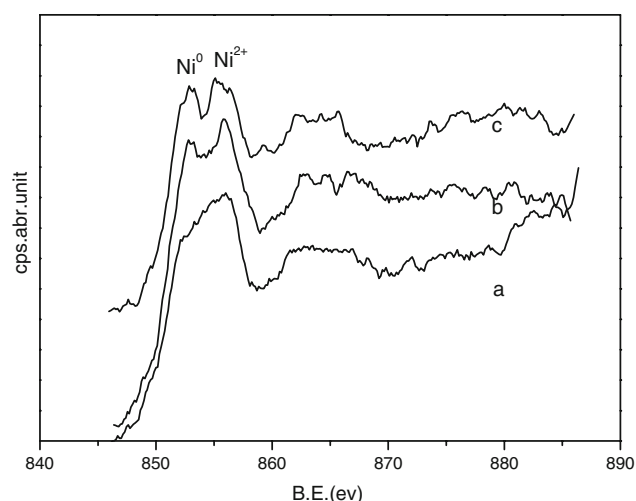


Fig. 7 XPS spectra of Ni ion on the surface of hexaaluminates $\text{LaNiAl}_{11}\text{O}_{19}$ and $\text{La}_{0.8}\text{A}_{0.2}\text{NiAl}_{11}\text{O}_{19}$ ($\text{A} = \text{Ce}, \text{Pr}$) after reduction A: a. Ce, b. La, c. Pr

Ni ions: 0 and +2. At the same time, as shown in Table 3, $\text{La}_{0.8}\text{Pr}_{0.2}\text{NiAl}_{11}\text{O}_{19}$ has the largest ratio of $\text{Ni}^0/\text{Ni}^{2+}$ after reduction. Therefore, it can be concluded that there are more Ni^0 ions in the Pr modified catalyst than in other two catalysts after reduction. And Ni^0 is the site of catalytic activity for the topic reaction. So, Pr can let more Ni^{2+} of the crystal lattice be reduced and enhance its catalytic activity.

Based upon the binding energies, it can also be confirmed that the oxidation states of the related ions in the samples are Ni^{2+} , Al^{3+} , O^{2-} , Pr^{3+} and Ce^{3+} , respectively.

3.5 Reducibility of Hexaaluminate $\text{La}_{0.8}\text{A}_{0.2}\text{NiAl}_{11}\text{O}_{19}$ Catalysts

Figure 8 shows the TPR profiles of $\text{LaNiAl}_{11}\text{O}_{19}$ and $\text{La}_{0.8}\text{A}_{0.2}\text{NiAl}_{11}\text{O}_{19}$ ($\text{A} = \text{Ce}$ or Pr). From the profiles we can find that each of these catalysts shows only one reduction peak, indicating that A-modified Ni-based hexaaluminates $\text{La}_{0.8}\text{A}_{0.2}\text{NiAl}_{11}\text{O}_{19}$ exhibit almost the same reduction profiles and need extremely higher reduction temperature than nickel oxide, which starts to be reduced at about 810 °C, meaning that hexaaluminates $\text{La}_{0.8}\text{A}_{0.2}\text{NiAl}_{11}\text{O}_{19}$ have reduction stability at higher temperature. At the same time, every sample of this series

Table 3 Binding energy of $\text{Ni}_{2p_{3/2}}$ on the surface of hexaaluminates $\text{La}_{0.8}\text{A}_{0.2}\text{NiAl}_{11}\text{O}_{19}$ ($\text{A} = \text{La}, \text{Pr}$ and Ce) (eV)

A	$\text{La}_{0.8}\text{A}_{0.2}\text{NiAl}_{11}\text{O}_{19}$	Ni_{2p}		$\text{Ni}^0/\text{Ni}^{2+}$
Pr	$\text{La}_{0.8}\text{Pr}_{0.2}\text{NiAl}_{11}\text{O}_{19}$	852.5	855.7	1.5
La	$\text{LaNiAl}_{11}\text{O}_{19}$	852.5	855.9	1.2
Ce	$\text{La}_{0.8}\text{Ce}_{0.2}\text{NiAl}_{11}\text{O}_{19}$	852.4	855.6	1.0

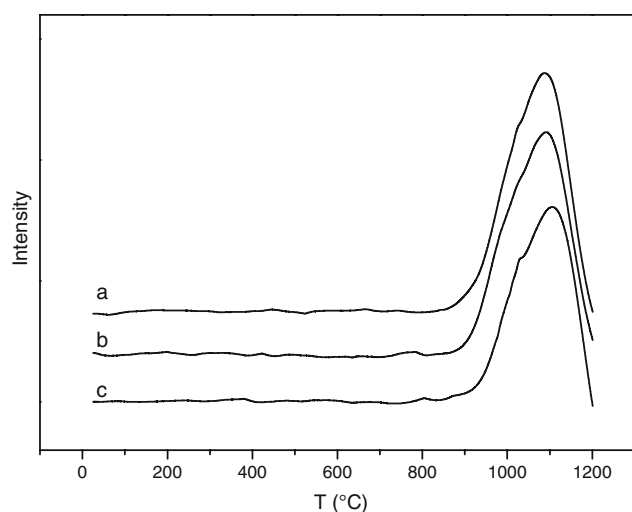


Fig. 8 TPR profiles of hexaaluminates $\text{LaNiAl}_{11}\text{O}_{19}$ and $\text{La}_{0.8}\text{A}_{0.2}\text{NiAl}_{11}\text{O}_{19}$ ($\text{A} = \text{Ce}, \text{Pr}$). *a.* Pr, *b.* La, *c.* Ce

of $\text{La}_{0.8}\text{A}_{0.2}\text{NiAl}_{11}\text{O}_{19}$ gives only one reduction peak, which does not drop down even up to 1,000 °C. The XRD patterns of the samples after reduction demonstrate that the reduced hexaaluminates still possess the same crystalline structure as that obtained before reduction. Based on the binding energies of Ni ions on the surface of the samples before reduction, it can be illustrated that the Ni ions inlaid in the hexaaluminate lattices are extremely stable and have only oxidation state Ni^{2+} and only a part of Ni^{2+} can be reduced to Ni^0 at high temperature. Besides, we can also observe that the reducibility of $\text{La}_{0.8}\text{A}_{0.2}\text{NiAl}_{11}\text{O}_{19}$ compounds is different due to the difference of modifiers.

Table 4 gives the data of the TPR profiles of $\text{LaNiAl}_{11}\text{O}_{19}$ and $\text{La}_{0.8}\text{A}_{0.2}\text{NiAl}_{11}\text{O}_{19}$ ($\text{A} = \text{Ce}, \text{Pr}$). It can be seen that the reduction temperature is changed slightly, but the reduction peak area of rare earth metal modified samples is changed obviously. The reduction temperature increases in the following order $\text{Pr} < \text{La} < \text{Ce}$, and the area size of reduction peak decreases in the order $\text{Pr} > \text{La} > \text{Ce}$. Therefore, it is indicated that Ce modified hexaaluminate $\text{La}_{0.8}\text{A}_{0.2}\text{NiAl}_{11}\text{O}_{19}$ gives the highest reduction temperature but the area size of the reduction peak is the least. Based on the above results, it can be concluded that the Ni ions in the lattice of Ce modified

hexaaluminate $\text{La}_{0.8}\text{Ce}_{0.2}\text{NiAl}_{11}\text{O}_{19}$ are more difficult to be reduced than that in the lattice of $\text{LaNiAl}_{11}\text{O}_{19}$ and Pr modified one. As known, the higher the reduction temperature, the stronger the interaction between the metallic ions in the lattice of hexaaluminates. Thus, based on the XPS data the above mentioned fact may be caused by the electron transformation between Ce^{4+} and Ce^{3+} during the reduction of $\text{La}_{0.8}\text{Ce}_{0.2}\text{NiAl}_{11}\text{O}_{19}$. As a result, Pr modified hexaaluminate $\text{La}_{0.8}\text{Pr}_{0.2}\text{NiAl}_{11}\text{O}_{19}$ gives the lowest reduction temperature than $\text{LaNiAl}_{11}\text{O}_{19}$, but the intensity of the peak area is increased with the Pr modified, meaning that more Ni^{2+} ions in the Pr modified sample can be reduced to metallic Ni^0 compared to that in $\text{LaNiAl}_{11}\text{O}_{19}$ at the same temperature. The characterization datas indicate that there are more Ni^{2+} ions to be reduced in the Pr modified hexaaluminate $\text{La}_{0.8}\text{Pr}_{0.2}\text{NiAl}_{11}\text{O}_{19}$.

From the TPR profiles, we can conclude that only Ni^{2+} ions can be reduced from the lattice when the reduction temperature is 900 °C, which gives a reasonable explanation of the fact that the active species for the reforming reaction is Ni^0 . And it can also be concluded that when Pr is employed as modifier, the Ni^{2+} ions in $\text{La}_{0.8}\text{Pr}_{0.2}\text{NiAl}_{11}\text{O}_{19}$ can more easily be reduced. Thereby, its activity for CO_2 reforming of CH_4 can be improved. The above mentioned fact illustrates that the reducibility of the hexaaluminates $\text{La}_{0.8}\text{A}_{0.2}\text{NiAl}_{11}\text{O}_{19}$ depends on the properties of transition metal Ni and is also affected by rare earth modifiers.

4 Conclusion

The interaction between Ni and La plays a very important role in the formation of the active phase of nickel and is mainly responsible for the activity of nickel based catalysts for the reaction of CO_2 with CH_4 . The Ni^0 , often formed as the major active phase in the hexaaluminate $\text{LaNiAl}_{11}\text{O}_{19}$ and $\text{La}_{0.8}\text{A}_{0.2}\text{NiAl}_{11}\text{O}_{19}$ ($\text{A} = \text{Ce}, \text{Pr}$) is considered to be responsible for the high catalytic activity. The hexaaluminate $\text{LaNiAl}_{11}\text{O}_{19}$ and $\text{La}_{0.8}\text{A}_{0.2}\text{NiAl}_{11}\text{O}_{19}$ ($\text{A} = \text{Ce}, \text{Pr}$) catalysts have been prepared, in which the transition metal Ni as active component is inlaid in the hexaaluminate lattices. These Ni species provide large surface areas, which can increase the reactivity and reduce the coking after reaction at high temperature. Substitution of La by Pr does not change the structure of the “bound-state” Ni species, facilitating electron transformation between Ni ions and La ions to maintain the Ni at a low valence, which would promote activation of the reactant and elimination of coking. The addition of Pr can accelerate the reduction of the Ni^{2+} ions in $\text{La}_{0.8}\text{Pr}_{0.2}\text{NiAl}_{11}\text{O}_{19}$. However, there is a redox of $\text{Ce}^{4+}/\text{Ce}^{3+}$ in $\text{La}_{0.8}\text{Ce}_{0.2}\text{NiAl}_{11}\text{O}_{19}$ during the reaction. Thereby, this redox bates the electron

Table 4 The data of TPR profiles of hexaaluminates $\text{La}_{0.8}\text{A}_{0.2}\text{NiAl}_{11}\text{O}_{19}$ ($\text{A} = \text{La}, \text{Pr}$ and Ce)

Catalyses	Data of TPR	
	Reduction temperature (°C)	Area
$\text{LaNiAl}_{11}\text{O}_{19}$	1,093	8,438
$\text{La}_{0.8}\text{Pr}_{0.2}\text{NiAl}_{11}\text{O}_{19}$	1,080	8,506
$\text{La}_{0.8}\text{Ce}_{0.2}\text{NiAl}_{11}\text{O}_{19}$	1,105	7,026

transformation between Ni and La ions. So Pr is a more valuable additive than Ce in the Ni-based catalysts for CH_4/CO_2 reforming, especially when it is employed as a modifier in the hexaaluminate $\text{La}_{0.8}\text{A}_{0.2}\text{NiAl}_{11}\text{O}_{19}$.

Acknowledgments The authors gratefully acknowledge the support of this work from NNSF China (20673047).

References

- Hou ZY, Yokota O, Tanaka T, Yashima T (2003) *Catal Lett* 87:37
- Slagtern A, Schuurman Y, Leclercq C, Verykios XE, Mirodatos C (1997) *J Catal* 172:118
- Liu BS, Au CT (2001) *Catal Lett* 77:67
- Vernon PDF, Green MLH, Cheetham AK, Ashcroft AT (1992) *Catal Today* 13:417
- Yamazaki O, Nozaki T, Omata K, Fujimoto K (1992) *Chem Lett* 10:1953
- Tsang SC, Claridge JB, Green MLH (1995) *Catal Today* 23:3
- Zhang Z, Verykios XE, MacDonald SM, Affrossman SJ (1996) *J Phys Chem* 100:744
- Therdthianwong S, Siangchin C, Therdthianwong A (2008) *Fuel Process Technol* 89:160
- Slagtern A, Olsbye U, Blom R, Dahl IM, Fjellvag H (1997) *Appl Catal* 165:379
- Wang S, Lu GQ (1998) *Appl Catal* 169:271
- Zhang JG, Wang H, Dalai Ajay K (2007) *J Catal* 249:300
- Iyi N, Takekawa S, Kimura S (1989) *J Solid State Chem* 83:8
- Machida M, Eguchi K, Arai H (1989) *J Catal* 120:377
- Groppi G, Cristiani C, Forzatti P (1997) *J Catal* 168:95
- Ji M, Bi Y, Zhen K, Wu Y (1997) *Chem J Chin Univ* 18:1698
- Ji M, Bi Y, Zhen K, Wu Y (1998) *Chem J Chin Univ* 19:1666
- Xu ZL, Zhen M, Bi YL, Zhen KJ (2000) *Catal Lett* 64:157
- Xu ZL, Zhen M, Bi YL, Zhen KJ (2000) *Appl Catal* 198:267
- Liu Y, Jiang PB, Cheng TX, Wang JX, Li WX, Bi YL, Zhen KJ (2003) *Catal Lett* 85:101
- Edwards JH, Maitra AM (1995) *Fuel Process Technol* 42:269
- Bradford MCJ, Vannice MA (1999) *Catal Rev Sci Eng* 41:1
- Machida M, Eguchi K, Arai H (1990) *J Catal* 123:477
- Yan L-C, Thompson LT (1998) *Appl Catal* 171:219
- Eguchi K, Inoue H, Sekizawa K, Arai H (1996). In: 11th International congress on catalysis—40th Anniversary, *Stud Surf Sci Catal.*, vol 101. Elsevier, Amsterdam, p 417
- Slagtern Á, Olsbye U, Blom R, Dahl IM, Fjellvag H (1996) *Appl Catal A* 145:375
- Xu ZL, Zhao LN, Pang F, Wang L, Niu C (2007) *J Nat Gas Chem* 16:60–63
- Oh YS, Roh HS, Jun KW (2003) *Int J Hydrogen Energy* 28:1387
- Chu Y, Li S, Lin J, Gu J, Yang Y (1996) *Appl Catal* 134:67
- Eguchi K, Inoue H, Sekizawa K, Arai H (1996). In: *Proceedings of the 11th International congress on catalysis—40th Anniversary*, Baltimore, MD, USA, June 30–July 5, *Stud Surf Sci Catal*, vol 101, Elsevier Science B.V., Amsterdam, p 417
- Xu Z, Li YM, Zhang JY, Liu C, Zhou RQ, Duan ZT (2001) *Appl Catal A Gen* 210:45–53
- Wang R, Xu HY, Liu XB, Ge QJ, Li WZ (2006) *Appl Catal A Gen* 305:204–210